11th World Congress on Computational Mechanics (WCCM XI)
5th European Conference on Computational Mechanics (ECCM V)
6th European Conference on Computational Fluid Dynamics (ECFD VI)
E. Oñate, J. Oliver and A. Huerta (Eds)

COMPUTATIONAL MODELING OF AN MRI GUIDED DRUG DELIVERY SYSTEM BASED ON MAGNETIC NANOPARTICLE AGGREGATIONS FOR THE NAVIGATION OF PARAMAGNETIC NANOCAPSULES

N.K. Lampropoulos*, E.G. Karvelas* and I.E. Sarris*

* Department of Energy Technology, Technological & Educational Institute of Athens, Agiou Spiridonos 17, 12210 Athens e-mail: nikolaoslampropoulos@hotmail.com , web page: http://www.teiath.gr/

Key words: MRI guided drug delivery, Aggregations, Magnetic nanocapsules

Abstract. A computational method for magnetically guided drug delivery is presented and the results are compared for the aggregation process of magnetic particles within a fluid environment. The model is developed for the simulation of the aggregation patterns of magnetic nanoparticles and for magnetic targeting under the influence of MRI magnetic coils and fluid flow. A novel approach for the calculation of the drag coefficient of aggregates is presented. The comparison with experimental and numerical results for the literature is showed that the proposed method predicts well the aggregations in respect to their size and pattern dependance, on the concentration and the strength of the magnetic field, as well as their velocity when particles are driven through the fluid by magnetic gradients.

1 INTRODUCTION

From the beginnings of 1970s researchers were studying the concept of Magnetic guided drug delivery [1, 2]. The concept is to attach the drug to the micro- or nanoparticles and then to inject them to the bloodstream. For the guidance to the targeted area, a Magnetic Resonance Imaging (MRI) is needed. By making use of the magnetic guided drug delivery method, the quantity of the drug required to reach therapeutic levels is being reduced. Also, the drug concentration at targeted sites is increased.

The efficiency of this concept depends on the materials of the particles, the blood flow rate and the intensity of the magnetic field [3]. A small size of particles implies a magnetic response of reduced strength and as a result, it is difficult to drive particles and keep them in the targeted region [4]. In order to overcome this difficulty the use of magnetic particles to create aggregations is proposed in order to increase the magnetic response [5]. When

the aggregations reach the targeted region, they break up into particles. The break up can be achieved by using superparamagnetic particles that lose the magnetization after moving from the magnetic field [5]. The size of aggregates is very important parameter, since a large aggregation could form clots in small arteries. On the other hand, a small aggregation would be dragged away from the cardiovascular system circulation. In addition, the magnetic field strength is limited in sites that are located inside the human body. That was the reason for implementation magnets near the targeted sites [6, 7].

Since an analytical study of aggregation process is impossible to be implemented, a numerical model for magnetically guided drug delivery is attended. The forces acting on a particle are described in detail in Section 2. The model is validated through a comparison with two benchmark test cases [5], [8] and the results are discussed in Section 3. Also, the capabilities of the model in magnetic targeting are described in this section. Finally, conclusions are presented in Section 4.

2 MODELING

For the propulsion model of the particles, four major forces are considered, i.e. the magnetic force from MRIs Main Magnet static field as well as the Magnetic field gradient force from the special Propulsion Gradient Coils. The static field caters for the aggregation of nanoparticles while the magnetic gradient navigates the agglomerations. Moreover,the contact forces among the aggregated nanoparticles and the wall is used. The Stokes drag force for each particle is considered, while only spherical particles are used here. And, finally gravitational forces due to gravity and the force due to buoyancy are added.

The motion of particles are given by the Newton equations.

$$m_i \frac{\partial \boldsymbol{u}_i}{\partial t} = \boldsymbol{F}_{mag\_i} + \boldsymbol{F}_{nc\_i} + \boldsymbol{F}_{tc\_i} + \boldsymbol{F}_{hydro\_i} + \boldsymbol{F}_{boy\_i} + \boldsymbol{W}_i \tag{1}$$

$$\boldsymbol{I}_i \frac{\partial \omega_i}{\partial t} = \boldsymbol{M}_{drag\_i} + \boldsymbol{M}_{con\_i} + \boldsymbol{T}_{mag\_i} \tag{2}$$

where the index i stands for the particle i. All quantities indicated in (1) and (2) are depicted in Figure 1.The bold variables are vectors.

In the following section, the forces that are taking into account during the simulation are described in detail

2.1 *Forces acting on particles*

1. *Magnetic Forces:* Magnetic forces $\boldsymbol{F}_{mag\_i}$ exerted on the i particle are given by [9–11] :

$$\boldsymbol{F}_{mag\_i} = \boldsymbol{F}_{intmag\_i} + \boldsymbol{F}_{ismag\_i} \tag{3}$$

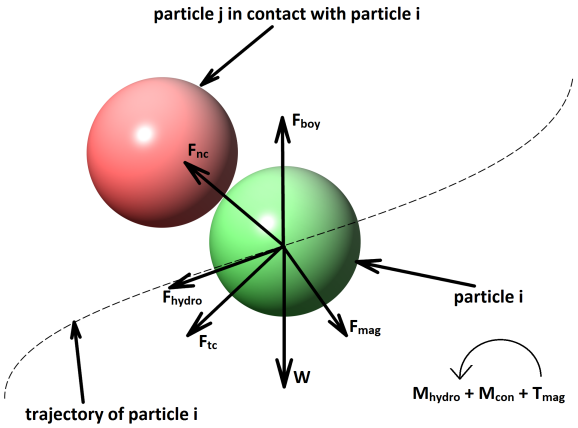

Figure 1: Forces and moments of a particle.

$\boldsymbol{F}_{intmag\_i}$ is the magnetic force due to the interaction of the ith particle with the magnetic field. $\boldsymbol{F}_{ismag\_i}$ are the magnetic forces acting on the ith particle due to its interaction with the surrounding magnetic particles.

The force $\boldsymbol{F}_{intmag\_i}$ is given by

$$\boldsymbol{F}_{intmag\_i} = V(\boldsymbol{m}_i \cdot \nabla)\boldsymbol{B}_{ext\_i} \tag{4}$$

The force $\boldsymbol{F}_{ismag\_i}$ is given by

$$\boldsymbol{F}_{ismag\_i} = \sum_{j}^{N} \boldsymbol{F}_{ismag\_ji} \tag{5}$$

The numerical model for the magnetic forces is given in [8].

2. *Fluid Forces:* Each particle is subjected to the fluid drag force. The drag force reads :

$$\boldsymbol{F}_{drag\_i} = \frac{1}{2}\rho u^2 C_d A \tag{6}$$

where ρ is the density of the fluid, u is the speed of the object relative to the fluid and A is the reference area which equals to πr^2, where r stands for the radius of spherical particle. C_d is the drag coefficient given by

$$\boldsymbol{C}_d = \frac{24\left[1 + 0.15Re^{0.687}\right]}{Re} \tag{7}$$

where Re is the Reynolds number based on the particle diameter [12].

In the present work, a new model is developed for the substitution of the reference area A in Eq. (6) with the effective area A_{new}. This substitution takes into account the fact that the downstream spheres of the chain lie partially in the wake of the upstream one, therefore the reference area A in Eq. (6) of each sphere must be reduced to each real area that is exposed to the flow. On this basis the area A_{new} can be calculated as follows :

(a) Sweep all spheres.

(b) Find the tangent sphere to the current one.

(c) A straight chain assumption considered where the sphere (1) is tangent only to two spheres namely the upwind and downwind. Sphere (2) which lies upstream to sphere (1) is found out by checking the inner product $3\vec{2} * (\vec{U}_{obj} - \vec{U}_{fluid})$ to be positive, see Figure 2-3. Where $\vec{U}_{obj}$ stands for the velocity of the sphere and $\vec{U}fluid$ stands for the velocity of the fluid

(d) Project the area of spheres (2 and 1) on the plane $\vec{U}_{obj} - \vec{U}_{fluid}$ that is cross sphere (2) at each center, see Figure 4. This yields into two intersected circles, as shown in Figure 5.

(e) Change to plane coordinate system $(2D)$.

(f) Calculate the overlapping area (white domain in Figure 5). The mathematical formula reads :

$$E_{overlapping} = domain(234) + domain(134) - E(1234) \tag{8}$$

(g) Substitute Eq. (6) with the equation

$$\boldsymbol{F}_{drag\_i} = \frac{1}{2}\rho u^2 C_d A_{new} \tag{9}$$

In this way, the real reference area A_{new} of sphere exposed to the flow, i.e.:

$$A_{new} = \pi {r_i}^2 - E_{overlapping} \tag{10}$$

is taken into account.

3. *Collision Forces:* Each particle interacts with other particles through contact. In our model we use the Discrete Element Method (DEM) to calculate the motion of particles [13]. The DEM is a numerical model capable of describing the mechanical behaviour of assemblies of spheres and computing the motion and shear effect of a large number of small particles. In DEM particles are approximated as rigid bodies and the interactions between them is explicitly considered [14].

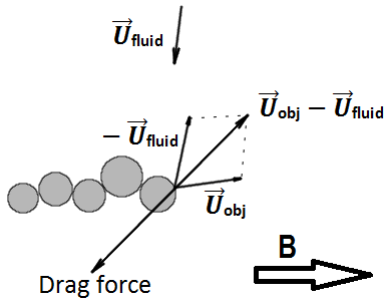

Figure 2: Relevant velocity and drag force of a particle.

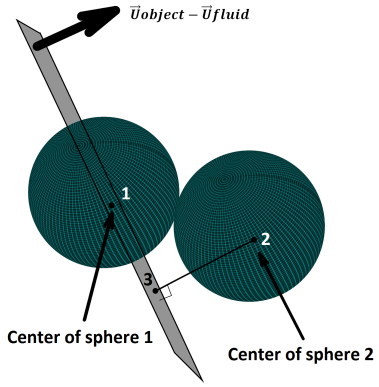

Figure 3: 3 (X_3, Y_3, Z_3) stands for the projection of sphere center 2 $(X_2, Y_2, Z_2))$ on the plane $\vec{U}_{obj} - \vec{U}_{fluid}$ crossing sphere 1 at each center (X_1, Y_1, Z_1).

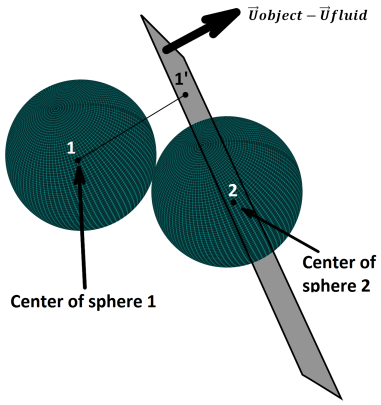

Figure 4: $1'$ $(X_{1'}, Y_{1'}, Z_{1'})$ stands for the projection of sphere center 1 $(X_1, Y_1, Z_1))$ on the plane $\vec{U}_{obj} - \vec{U}_{fluid}$ crossing sphere 2 at each center (X_2, Y_2, Z_2).

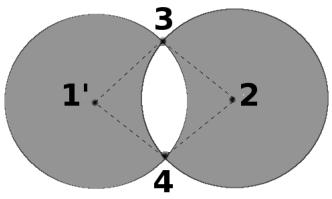

Figure 5: Circular sector of two spheres $E_{overlapping} = domain(234) + domain(134) - E(1234)$.

4. *Body Forces:* Only gravity and buoyancy are being included in the calculation of the body force. The force is addressed by

$$\boldsymbol{F}_{grav\_i} = \boldsymbol{W}_i + \boldsymbol{F}_{boy\_i} = \frac{4}{3}\pi r_i^3(\rho_i - \rho_f)\boldsymbol{g} \tag{11}$$

where ρ_i and ρ_f are the density of the particle i and the fluid, respectively, r_i is the radius of the particle i and $\boldsymbol{g}$ is the acceleration due to gravity.

2.2 *Magnetic Field and Interaction Domain*

The magnetic field $\boldsymbol{B}$ in the MRI bore is given by

$$\boldsymbol{B} = \boldsymbol{B}_0 + \tilde{\boldsymbol{G}} + \boldsymbol{B}_1 \tag{12}$$

where $\boldsymbol{B}_0$ is the MRI superconducting magnet field that is constant and uniform, $\tilde{\boldsymbol{G}}$ is the gradient field and $\boldsymbol{B}_1$ is the time dependent radio frequency field [15].

The magnetic interaction forces are inversely proportional to the fourth power of the separation distance [16, 17]

$$\boldsymbol{F} \propto \frac{M_i M_j}{(h + a_i + a_j)^4} \tag{13}$$

where F is the interaction force between two spheres in the parallel direction to B_0. M_i and M_j is the magnetic moments of the center of each sphere and h is the nearest distance between the surfaces of two spheres with radii a_i and a_j.

Although, a weak interaction is being observed for particles that are more than five radii apart, as time goes by, the interaction force is getting stronger, because the particles are getting closer to each other. Each particle interacts with all the other which are in the same area. The magnetic interaction domain is defined by the area of the domain that the particles are located in. This is a time consuming method, because every time the magnetic moments of all particles are calculated. In order to accelerate the method, we calculate the magnetic moments that are exerted on particle i from particles that are located in distance of 15 diameter. Then, only the magnetic moments that are located in distance of 10 diameter are stored in array. In this way, the magnetic moments of particles that are located in distance of 10 diameter are automatically recalled from the array in order to be used for the calculation of the magnetic moments of other particles.

Table 1: Simulation Results

Comparison of experimental with simulation results				
Concentr. mg/ml	Mean length (μm) ***simulation***	Standard Dev. ***simulation***	Mean length (μm) ***experiment***	Standard Dev. ***experiment***
0.563	34.02	23.72	31	16
1.125	59.14	43.19	59	36
2.25	108.93	83.79	137	85
4.5	201.49	109.42	317	195

2.3 *Numerical Method*

The OpenFoam platform was used in order to calculate the flow field and the uncoupled equations of particles motion [13]. The simulation process reads as follows: Firstly, the fluid flow is found using the pressure correction method. Upon finding the flow field (pressure, velocity) the motion of particles is evaluated by the Lagrangian method by solving Eq. (1) and (2) along the trajectory of each particle. The equations are solved in time by the Euler time marching method. The stability of the algorithm is guaranteed through time step of $10^{-6}s$. The spacing of the computational grid is equal to the diameter of the particles that were simulated.

3 Validation and discussion

Two test cases mentioned above, were simulated in order to validate the proposed method. The first one, which is described in Ref. [5], investigates the aggregation of particles dispersed in a stationary distilled water under the influence of a constant magnetic field. The diameter of each Fe_3O_4 particle was 11 μm. Solutions with particle concentrations of 0.563 mg/ml, 1.125 mg/ml, 2.25 mg/ml and 4.5 mg/ml were simulated under a uniform transverse magnetic field of $B_0 = 0.4$ T. No external magnetic gradient is applied during this experiment. The initial positions of the microparticles are randomly generated. At the beginning of each simulation for t=0s the magnetic field is B_0=0 T. Under the influence of a uniform magnetic field B_0=0.4T the particles (magnetic dipoles) are formed into chains and parallel to the uniform magnetic field within $t = 5ms$. In this case, there is no fluid flow and the density of the particles is bigger than the density of the fluid. Due to the external magnetic field and the magnetic properties of the particles, the particles are acting like magnets. As a result, the movements of the particles are attributed to gravity and magnetic interactions between the particles.

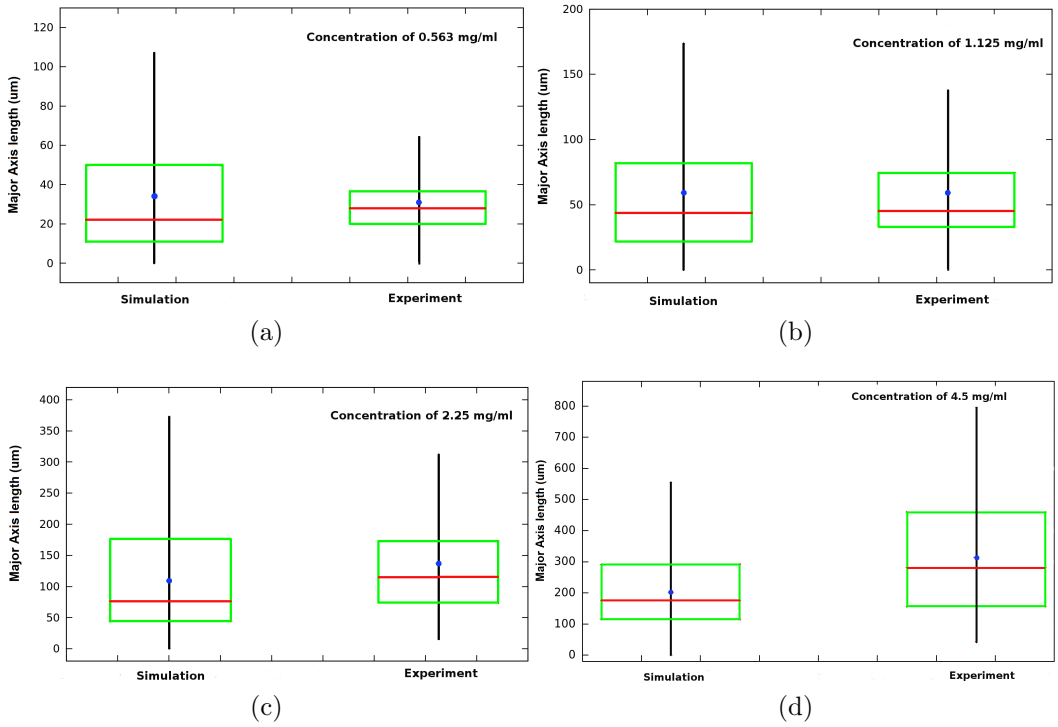

Figure 6: Box plots) show variations in the major axis length of aggregates .The boxes captures the lower quartile, median (red line) and upper quartile values. The black line that extended from the box show the upper and the lower fence. The blue dots shows the average length of the aggregations in each case. (a) Concentration =0.563 mg/ml (b) Concentration =1.125 mg/ml, (c) Concentration =2.25 mg/ml and (d) Concentration =4.5 mg/ml

The results from the simulation are compared to the experimental data of Ref. [5] as Figure 6 is showed. There is a small difference in terms of aggregation size as is depicted in Table 1.

The second test case, which is described in details in Ref. [8], investigates the flow and aggregation of particles under the combine action of a constant and a gradient external magnetic field acting together. A magnetic suspension of Polysterene magnetic particles ($5.5\mu m$) with density of $1050kg/m^3$ and concentration of $25kg/m^3$ was simulated in distilled water [8]. At the beginning of the simulation for t=0s the uniform magnetic field is B_0=0 T and the gradient magnetic field is $\tilde{G}$ =$0T/m$. Inside the fluid domain 100 particles are randomly placed. Under the combined application of a uniform magnetic field of intensity $B_0 = 0.005T$ and a magnetic gradient along the x-axis of $\tilde{G} = 1.4T/m$ the microparticles are successively aggregated as Figure 8 shown while at the same time they are transported in the direction

Table 2: Comparison of experimental and simulation results for Case 2

Parameters	Mean size (*particles*)	Std size (*particles*)	Mean velocity ($\mu m/s$)	std velocity ($\mu m/s$)
Experiment	7	5	7.5	1
Simulation	5.26	1.89	8.3	1.40

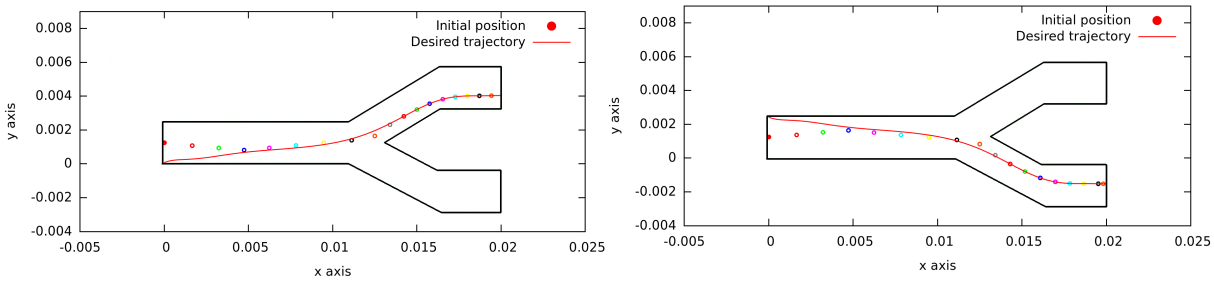

(a) (b)

Figure 7: Positions of particle under variable magnetic field in order to follow the desired trajectory

of the magnetic gradient. The results of the simulation are compared against the experimental data of Ref [8] in Table 2.

The third case, investigates the capabilities of the platform in magnetic driving. A y-shaped fluidic channel with a rectangular cross-section (length = 20 mm, width = 2.5 mm, depth = 0.3 mm) was simulated. The main branch of the channel was oriented along the x axis. The outlet branches had angle of 60 degrees with respect to the x axis. The velocity of flow has an average value of 12.2 mm/s and 6.1 mm/s in the main branch and in the outlet branches of the channel. Two trajectories were designed inside the domain. The first one, begins from the bottom of the inlet and ends to the upper branch, while the second one begins from the upper side of the inlet and ends to the lower branch, as is depicted in Figure 7. At t=0 s a particle was injected in the inlet of the domain. Then, the model calculates the forces that are exerted on the particle, the distance from the desired trajectory and estimates the appropriate value of the gradient magnetic field in order to move the particle towards to the desired trajectory. Using the appropriate value of the gradient magnetic field the distance between the particle and the desired trajectory is minimised, as is depicted in Figure 7 and tabulated in Table 3.

Table 3: Magnetic field in each time step in order to follow the particle the desired trajectory

Position	Time (s)	Magnetic Field (mT/m) (a)	Magnetic Field (mT/m) (b)
Initial	0	0	0
1	0.1	-300.17	303.81
2	0.2	-300.08	295.30
3	0.3	-282.80	219.12
4	0.4	300.66	-299.73
5	0.5	300.42	-295.85
6	0.6	300.36	-300.55
7	0.7	300.42	-300.29
8	0.8	300.65	-302.33
9	0.9	300.20	-298.92
10	0.10	-299.93	170.29
11	0.11	-208.32	78.41
12	0.12	-162.12	-9.94
13	0.13	-72.17	-83.27
14	0.14	51.99	-61.10
15	0.15	32.90	-37.07
16	0.16	24.95	-48.56
17	0.17	43.71	9.25

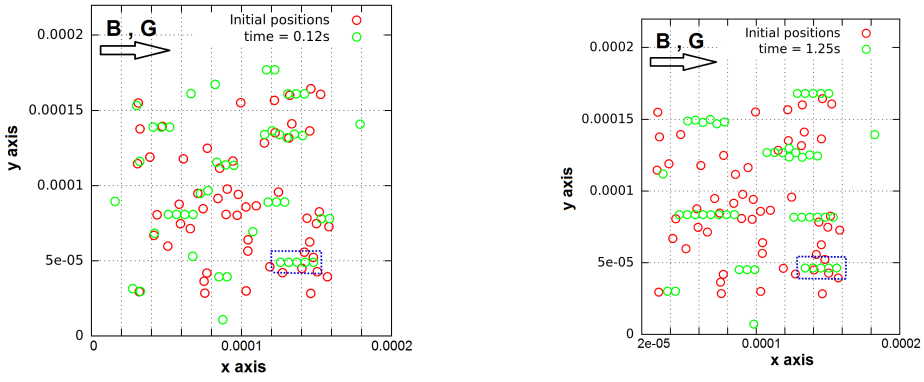

(a) (b)

Figure 8: Initial positions of particles (red circles). Particles displacement between consequent times (a) from $t = 0s$ to $t = 0.12s$, (b) from $t = 0s$ to $t = 1.25s$ of each particle.

4 Conclusion

A computational method for magnetically guided drug delivery was developed in order to predict the behaviour of magnetic particles for medical applications. This method aims at predicting the aggregation's procedure and the velocity of each particle inside the arteries and arterioles of a human body. It aims also at simulating the motion of aggregations when these are driven by MRI magnetic gradient coils.

The computational platform was tested through comparison with experimental and numerical data. It was shown that in a stationary fluid under a steady magnetic field, the current method can simulate satisfactory the experiments.

Furthermore, the model was used to move the aggregated particles under the influence of a constant and a superimposed gradient magnetic field. The results were in relative conformity with the experimental data in terms of velocity) while at the same time the results of the computational model present a difference in terms of aggregation size due to the small number of the used particles. In addition, the computational platform was used to lead a particle into a desired trajectory. The results from this simulation show that the method succeed to lead a particle into a desired trajectory. However, for leading more particles further development is needed.

REFERENCES

[1] A. Senyei, K. Widder, and C. Czerlinski, "Magnetic guidance of drug carrying microspheres," *Appl. phys.*, vol. 49, pp. 3578–83, 1978.

[2] K. Widder, A. Senyei, and G. Scarpelli, "Magnetic microspheres : a model system of site specific drug delivery in vivo." *Proc. Soc. Exp. Biol. Med.*, vol. 158, pp. 141–6, 1978.

[3] K. Widder, P. Marino, R. Morris, and A. Senyei, *In: Targeted Drugs, Goldberg E (Ed.).* NY, USA: John Wiley and Sons, 1983.

[4] Q. Pankhurst, J. Connolly, S. Jones, and J. Dobson, "Applications of magnetic nanoparticles in biomedicine," *Physiscs D:Applied Physics*, vol. 36, pp. 166–181, 2003.

[5] J.-B. Mathieu and S. Mantel, "Aggregation of magnetic microparticles in the context of targeted therapies actuated by a magnetic resonance imaging system," *J. Appl. Phys.*, vol. 106, p. 044904, 2009.

[6] T. Kubo, T. Sugita, and S. Shimose, "Targeted delivery of anticancer drugs with intravenously administreted magnetic lipomes in osteosarcoma- bearing hamsters," *Int. J. Oncol.*, vol. 17, pp. 309–16, 2000.

[7] B. Yellen, Z. Forbes, and D. Halverson, "Targeted drug delivery to magnetic implants for therapeutic applications," *Magn. Magn. Mater*, vol. 293, pp. 647–54, 2005.

[8] P. Vartholomeos and C. Mavroidis, "In silico studies of magnetic microparticle aggregations in fluid enviroments for MRI-guided drug delivery," *IEEE transactions on biomedical engineering*, vol. 59, no. 11, pp. 3028–3038, Nov. 2012.

[9] K. W. Yung, P. B. Landecker, and D. D.Villani, "An analytic solution for forces between two magnetic dipoles," *Magn. Elect. Sep.*, vol. 20, pp. 39–52, 1998.

[10] E. Climent, M. Maxey, and G. E.Karniadakis, "Dynamics of self-assembled chaining in magnetorheological fluids," *Langmuir*, vol. 20, pp. 507–513, 2004.

[11] J. D. Jackson, *Classical Electrodynamics,3rd ed.* Hoboken,NJ: Wiley, 1999.

[12] M. Karimi, G. Akdogan, K. H. Dellimore, and S. M. Bradshaw, "Comparison of different drag coefficient correlations in the cfd modelling of a laboratory-scale ruschton-turbine flotation tank," 2012.

[13] (2013, Jul.). [Online]. Available: http://www.openfoam.org

[14] E. Tijskens, H.Ramon, and J. Baerdemaeker, "Discrete element modelling for process simulation in agriculture," *J. of Sound and Vibration*, vol. 266, pp. 493–514, 2003.

[15] C. L. Epstein and F. W. Wehrli. (2005) Magnetic resonance imaging. [Online]. Available: http://www.math.upenn.edu

[16] A. Mehdizadeh, R. Mei, J. F. Klausner, and N. Rahmatian, "Interaction forces between soft magnetic particles in uniform and non-uniform magnetic fields," *Acta Mechanica Sin.*, vol. 26, pp. 921–929, 2010.

[17] T. Fujita and M. Mamiya, "Interaction forces between nonmagnetic particels in the magnetized magnetic fluid," *J. of Magnetism and Magnetic Materials*, vol. 65, pp. 207–210, 1987.